

# IMPACT OF EXPERIMENTAL CONDITIONS ON AUTOCORRELATION BUNCHLENGTH MEASUREMENTS \*

C. Settakorn, ChiangMai University, ChiangMai, 50200, Thailand  
 H. Wiedemann, Stanford University and SSRL, CA, 94305, USA

## Abstract

Bunch length measurements based on autocorrelation of coherent transition radiation emitted by short electron pulses have been implemented in many facilities in recent years. Since information of bunch length is based on the coherent transition radiation spectrum, any effect that might perturb the spectrum must be analyzed. In this paper, we present impact of experimental conditions that should be included in the bunch length analysis. A brief summary of beam splitter effects will be reviewed. New investigations on the pulse broadening due to dispersion in humid air, effects of a pyroelectric detector, and effects of beam sizes on the measurement will be discussed.

## 1 INTRODUCTION

The ability to measure electron bunch length well below picosecond is crucial for the progress to produce ultra short electron and radiation pulses as desired for future linear colliders, FELs or generation of coherent radiation. At SUNSHINE (Stanford UNiversity SHort INTense Electron source), we measure bunch lengths using coherent transition radiation emitted at wavelengths longer than or equal to the bunch length. By analyzing the autocorrelation of coherent transition radiation (TR), the bunch length can be determined [1]. The basic methods and experimental technique has been described in Refs. [2,3] including the effects of thin film beam splitter on the bunch length measurement. This paper covers some issues regarding the technique and data analysis that have been investigated in more detail [4]. These issues include effects of the pyroelectric detector, dispersion of the radiation pulse as it propagates through humid air, and effects of beam sizes.

## 2 BASIC PRINCIPLE

When accelerated, an electron bunch emits coherent radiation at wavelengths comparable to and longer than the bunch length. The coherent radiation spectrum is determined by the spectral distribution of the particular radiation emission process used and the particle distribution. The spectral distribution of TR generated from a vacuum-metal interface is frequency independent within our spectral range of interest. Therefore, the coherent TR spectrum is determined solely by the particle distribution.

$$I_{CTR}(\omega) = N_e^2 I_{TR} f(\omega) \quad (1)$$

\* Work supported by DOE # DE-AC03-76SF00515

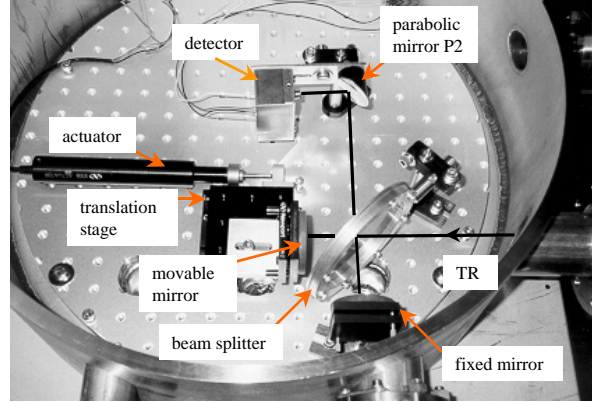


Figure 1: In-vacuum Michelson interferometer.

where  $N_e$  is the number of electrons in a bunch and  $f(\omega)$  is the form factor defined as the Fourier transform of the bunch distribution squared.

A spectral distribution of the coherent TR can be obtained using a Michelson interferometer, from which the detector signal as a function of the optical path difference, called interferogram  $I(\delta)$ , is recorded. This Fourier transform of the interferogram, which is the autocorrelation of the radiation pulse, is the radiation power spectrum. An interferogram of the coherent TR emitted from the electron bunch represents directly the autocorrelation of the particle distribution. The bunch length can then be derived from the interferogram [2].

## 3 IN-VACUUM BUNCH LENGTH MEASUREMENT

An in-vacuum Michelson interferometer was assembled to separate the effect of water absorption from other effects in the measurements. The interferometer is set up in a vacuum chamber which is connected to the main beam line. A picture of the in-vacuum Michelson interferometer is displayed in Fig. 1 showing its components.

Figure 2 shows an interferogram and radiation spectrum obtained from the in-vacuum Michelson interferometer. The radiation spectrum taken in vacuum is free from water absorption lines. The spectrum is not smooth as we first expected but clearly displays a periodic structure which could possibly be an outcome of interferences. The signatures in the interferogram also suggest that multiple reflections might occur. Since the thin film interference of a 25- $\mu\text{m}$  Kapton beam splitter features zero efficiencies

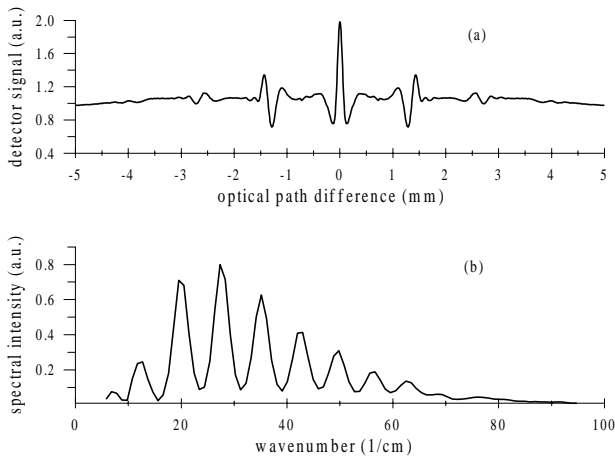


Figure 2: (a) interferogram and (b) radiation spectrum taken from the in-vacuum Michelson interferometer.

at  $112 \text{ cm}^{-1}$  interval [4], the features observed here do not originate from the beam splitter but is a feature of the pyroelectric detector used in the measurement.

### 3.1 Internal Reflection in a Pyroelectric Crystal

The Molecron P1-65 detector is made of a  $100 \mu\text{m}$  thick  $\text{LiTaO}_3$  pyroelectric crystal. The P1-65 has a metallic coating containing chromium applied to the front surface of the crystal to increase the response time [5]. The rear surface is also coated with a chromium layer and a heavy layer of gold which absorbs radiation through the visible region to  $1 \mu\text{m}$  [6]. The schematic diagram in Fig. 3(a) shows the structures of the pyroelectric sensor.

For far-infrared radiation, such as our radiation pulses, a fraction of radiation at the front surface is either reflected, absorbed, or preferably transmitted through the chromium coating [4]. Part of the transmitted radiation may later be reflected by the gold layer at the rear surface as shown schematically in Fig. 3(b). At unequal optical path lengths in the interferometer, part of the radiation from one arm is reflected on the rear surface of the crystal and travels toward the front surface. This reflected radiation can interfere with the radiation coming later from the longer arm of the interferometer. This leads to frequency dependent reflection or absorption of the detector as evident from the signatures in the interferogram and the spectrum.

In Fig. 3(a), the main peak (center peak) is the result of the autocorrelation of the radiation pulse while the other signatures are cross-correlations of the radiation pulse and reflected pulses. Cross-correlation can occur when a radiation pulse from one arm is reflected on the rear surface of the crystal and then interferes with the radiation pulse coming from the longer arm. Evidence of many cross-correlations confirm that multiple reflections within the detector crystal can occur.

To support the above explanation, test measurements were conducted with a Molecron P1-62 detector which is

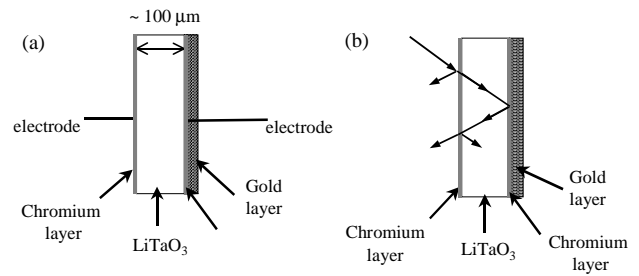


Figure 3: Schematic diagrams show (a) structures of the pyroelectric detector and (b) the radiation reflection/absorption mechanism.

constructed in a similar way as the Molecron P1-65 but the pyroelectric crystal is only  $25 \mu\text{m}$  thick (courtesy of Molecron Detector, Inc. as a test sample). The interferogram when using the P1-62 detector features cross-correlations closer to the main peak and the periodic-like spectrum has larger interval [4] as expected and supporting multiple reflections in the detector crystal.

As long as the cross-correlation signatures do not merge into the main peak, the pyroelectric detector, such as the P1-65 detector, can be used for bunch length measurements.

### 3.2 Dispersion in Humid Air

To study effects of humidity in ambient air on the bunch length measurement, we compare interferograms taken in air and in vacuum. After taking bunch length measurements in vacuum, the interferometer is opened up to the atmospheric environment. The measurements in air are then taken. Interferograms for both cases are shown in Fig. 4, displaying the increase of the interferogram width for the measurement in the air. The average FWHM of the interferograms measured in vacuum is  $87 \pm 2 \mu\text{m}$  while the measurements in the air give an average FWHM of  $101 \pm 3 \mu\text{m}$ . Applying the correction from low frequency suppression due to beam splitter and mirror diffraction [4], the corrected bunch lengths for both measurements can be obtained. The corrected FWHM for the in-vacuum measurement is  $126 \mu\text{m}$ , while that of the in-air measurement is  $158 \mu\text{m}$ , which is  $32 \mu\text{m}$  longer. This broadening can be explained by dispersion due to water vapor in humid air. Since the refractive index of humid air is not constant over the far-infrared regime, different frequencies propagate with different velocities. Consequently, the radiation pulse is spreading, as it travels through the air.

Estimate of the pulse spreading using the variation of the group velocity in air (ignoring narrow absorption bands) evaluated from the refractive index of humid air data in Ref. [7] fits well to the observation. It is worth noting that the pulse spreading depends on the radiation spectral range. For example, a long bunch generating coherent radiation within mm-wavelengths will not be vulnerable to

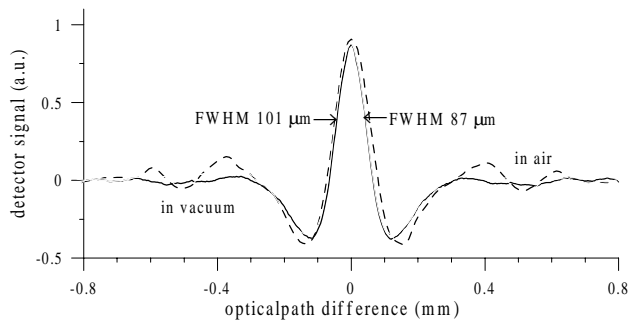


Figure 4: Comparison of the interferograms taken in vacuum and in humid air.

the dispersion since the group velocity variation within the radiation spectral range is very small. A very short bunch, on the other hand, generates a broad spectrum and is subjected to large pulse spreading when it traverses the humid air. In any case, to avoid the pulse spreading and for precise bunch length measurements, either the interferometer must be placed under vacuum or corrections must be applied.

#### 4 EFFECT OF BEAM SIZE

Perturbations of the coherent radiation spectrum due to interference effects from an extended source size also disturbs the bunch length measurement. In general, it is important to minimize the contribution of transverse distribution to fully obtain the coherent spectrum that is determined solely by the longitudinal particle distribution.

The experiment to investigate effects of beam size on the bunch length measurement has been conducted. The bunch lengths are measured as a function of beam size. The beam size is varied using a pair of quadrupole magnets located 60 cm upstream from the radiator and is measured by analyzing an image of the beam on the fluorescent screen mounted behind the radiator. The image of the beam is analyzed to give horizontal and vertical beam profiles. Interferograms of the coherent TR, generated from the electron beams focused to different beam sizes, are recorded using the in-vacuum Michelson interferometer. The FWHM of each interferogram gives us a measured value  $\sigma_m$  associated with each beam size in the measurement. In most of the cases, the beam has an oblong beam cross section with a larger height than width ( $\sigma_y > \sigma_x$ ) and therefore the beam size will be represented by the effective beam width  $\sigma_\rho$  where  $\frac{1}{2}(\sigma_x + \sigma_y) < \sigma_\rho < \sigma_y$  [4].

The experimental results are shown in Fig. 5 with the effective beam sizes bounded by the two limits and the measured bunch lengths  $\sigma_m$  are within  $\Delta\sigma_m \approx 3 \mu\text{m}$ . As the beam size decreases, the measured bunch length becomes smaller. The measured values should approach the real bunch length when the beam size is small enough so that the contribution of the transverse distribution becomes negligible compared to that of the longitudinal distribution. In our measurement, the beam sizes can not be focussed

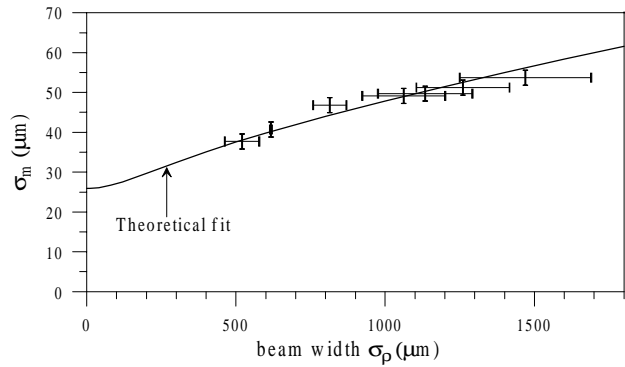


Figure 5: Measured bunch length  $\sigma_m$  as a function of beam size.

small enough to be in that regime. This focussing limitation is due to the energy droop along a macropulse, i.e. the beam size varies along the macropulse.

The theoretical estimation of the bunch length as a function of the beam size is shown by the solid line. The calculation was evaluated for the transition radiation generated by a 26 MeV monochromatic beam, collected over an acceptance angle of  $\pm 160$  mrad. The trend in the experimental results and the calculation suggest that the bunch length  $\sigma_z$  is about  $26 \mu\text{m}$ .

For a precise bunch length measurement, it is important to focus the beam well to achieve a small beam size at the radiator so that the transverse distribution is negligible. Bunch length measurement as a function of beam size, similar to what has been done in this experiment, can be used to separate longitudinal and transverse contribution for more accurate estimate of the bunch length.

#### 5 REFERENCES

- [1] W. Barry in *Proceeding of Workshop on Advanced Beam Instrumentation*, Tsukuba, Japan, 1991, KEK Proceeding 92-1, p.224.
- [2] H. Lihn, P. Kung, C. Settakorn, and H. Wiedemann, *Phys. Rev. E*, **53**(6), 6413 (1996).
- [3] H. Lihn, *Stimulated Transition Radiation*, PhD Thesis, Stanford University, California, 1996.
- [4] C. Settakorn, *Generation and Use of Coherent Transition Radiation from Short Electron Bunches*, PhD Thesis, Stanford University, California, 2001.
- [5] W. B. Tiffany, "The amazing versatile pyroelectric", Tech. Rep., Molelectron Detector, Inc., Oregon.
- [6] C. B. Roundy, *Advance in Pyroelectric Detectors*, PhD Thesis, Stanford University, California, 1973.
- [7] J. R. Birch, A. J. Kemp and M. N. Afsar, *Infrared Phys.*, **18**, 827 (1997).